Exploring the Stability of Golden Fullerenes

3 **AUTHORS**, INCLUDING:

Juha Vaara

University of Oulu

136 PUBLICATIONS   **2,888** CITATIONS

SEE PROFILE

Dage Sundholm

University of Helsinki

205 PUBLICATIONS   **4,652** CITATIONS

SEE PROFILE

Exploring the Stability of Golden Fullerenes

Mikael P. Johansson, Juha Vaara, and Dage Sundholm

More About This Article

Additional resources and features associated with this article are available within the HTML version:

- Supporting Information
- Access to high resolution figures
- Links to articles and content related to this article
- Copyright permission to reproduce figures and/or text from this article

View the Full Text HTML

Exploring the Stability of Golden Fullerenes

Mikael P. Johansson,*,† Juha Vaara,‡ and Dage Sundholm§

Lundbeck Foundation Center for Theoretical Chemistry, Aarhus University, Langelandsgade 140,
DK-8000 Aarhus C, Denmark, Laboratory of Physical Chemistry and Laboratory for Instruction in Swedish,
Department of Chemistry, University of Helsinki, P.O. Box 55, FI-00014 Helsinki, Finland

Received: September 11, 2008; Revised Manuscript Received: October 14, 2008

The golden fullerenes Au_{32}, Au_{50}, and Au_{72} are reinvestigated, using high-level relativistic density functional theory (DFT). Their stability is found to be highly dependent on the electron count fulfilling the criterion of spherical aromaticity, which in turn is sensitive to relativity. Only neutral and cationic Au_{32} are shown to be stable with respect to alternative, space-filling isomers. Endohedrally doping Au_{32} with an alkali metal cation significantly increases its thermal stability, facilitating experimental preparation of the hollow cluster.

1. Introduction

A few years ago, an intriguing new class of gold nanoclusters was proposed: The hollow golden fullerenes.[1,2] The stability of the Au_{32} fullerene was attributed to spherical aromaticity,[1] with its 32 outer 6s electrons fulfilling the $2(N + 1)^2$ rule.[3] Subsequently, two other spherically aromatic golden balls were proposed to be stable, Au_{50}[4,5] and Au_{72}.[6] In the other size direction, the tetrahedral dianion Au_{16}^{2-} also fulfils the $2(N + 1)^2$ rule.[7] To date, however, the largest experimentally observed, pure hollow structure is Au_{18}^-.[8] While the free Au_{32}^- anion has been shown to be a space-filling lump,[9] hollow Au_{32} has been prepared but so far only immersed in organic ligands.[10] In what follows, we explore the reasons for the puzzling lack of direct observation of the larger golden fullerenes, in spite of their theoretically proposed high stabilities. We will show that maintaining spherical aromaticity is crucial and investigate the relativistic influence on aromatic character. Finally, we propose a way of detecting the hollow form experimentally.

The basis for this investigation will be the use of a sufficiently high level of theory. It was recently shown that density functionals traditionally used in the study of gold clusters have a surprisingly strong bias toward planar structures and are thus unsuitable for a quantitative assessment of relative energies.[11] The underestimation of the aurophilic attraction[12] leads to a corresponding underestimation of the stability of compact isomers that have more bonding neighbors per atom. To establish a more correct energy ordering between open and space-filling geometries, the use of functionals which provide a good description of the Au–Au interaction and surface energies is necessary. As the hollow clusters can be considered to be pseudoplanar, it is reasonable to expect that also their stability has been overestimated compared to alternative isomers in practically all previous studies.

2. Methods

The main computational method used is the nonempirical meta-generalized gradient approximation (mGGA) functional by Tao, Perdew, Staroverov, and Scuseria (TPSS).[13] It has

recently been shown that this functional is superior to other functionals free of empirical corrections in describing van der Waals interactions and transition metal systems[14,15] and outperforms others in describing Au–Au interactions[11] The non-locality introduced into the description via the kinetic energy density dependence (and thus orbital dependence), combined with a good description of jellium surface energies, are apparently important. There is naturally still room for improvement for the long-range correlation regime within the DFT framework.

All structures have been (re)optimized with the TPSS functional, using the split-valence basis set def2-SVP(4p).[16] (4p) denotes that the p-function with an exponent of ~0.8 has been decontracted from the block of 4p-functions of the original def2-SVP basis set. This significantly improves the quality of the basis set.[11] Scalar-relativistic effects were accounted for via the use of the relativistic Stuttgart 1990 pseudopotential.[17] Also the vibrational frequencies were computed at the same level of theory. Zero-point vibrational energies and free energy (ΔG) corrections were computed from the unscaled harmonic frequencies, which were obtained numerically. The thermal corrections to ΔG assumed ideal gas behavior, treating rotation classically. A large basis set is necessary to avoid intramolecular basis set superposition error, which otherwise artificially stabilizes compact isomers,[11] so the final energies were evaluated with the doubly polarized quadruple-ζ basis set, def2-QZVPP.[16]

Two-component spin–orbit (SO) corrections were calculated with the PBE functional[18] and the def2-QZVPP-2c extended basis set, which accounts for the spatial splitting of inner p-shells, and a corresponding two-component pseudopotential.[19] The correction was taken as the difference between the PBE energies including and excluding SO effects.

The magnetic shielding and NICS[20] values were also calculated at PBE level, using the Stuttgart 1990 pseudopotential and the original valence basis set.[17] For sodium, the TZVP basis set[21] was used.

The geometry optimizations and energies were calculated with the Turbomole V5-10 package,[22−26] with the exception of the PBEsol[27] single-point energies, for which a suitably modified version of the NWChem 5.0 package[28] was used. The magnetic shieldings were calculated with the Gaussian 03 package.[29] Default convergence and threshold parameters were used, with the following, tighter exceptions: The Turbomole calculations used the "m4" type grid[30] and a self-consistent field (SCF)

TABLE 1: Energy Difference (in kJ/mol) between the Hollow and Representative Compact Forms of Au_{50} and Au_{72}[a]

	neutral	cation	anion
Au_{50}	+73	+112	+110
Au_{72}	+253	+331	+244

[a] Positive energies indicate that the hollow forms are less stable.

TABLE 2: Relative Energies (in kJ/mol) of the Hollow and a Compact Form of Au_{32}[a]

	neutral	cation	anion
SR	−43.25	−15.68	+36.42
SO	+11.77	−9.55	−4.31
ZPE	+3.09	+3.08	+2.58
total	−28.4	−22.2	+34.7

[a] Positive energies indicate that the hollow form is less stable. Scalar-relativistic electronic energies (SR), spin-orbit corrections (SO), and zero-point vibrational energies (ZPE) are summed for the final energy differences.

convergence criterion of 10^{-7} Hartree ("m5" grid and SCF convergence 10^{-8} Hartree in connection with the numerical second derivatives); the geometry optimizations used a gradient norm convergence of 10^{-4}; and the Gaussian calculations used the "tight" SCF convergence setting.

3. Results and Discussion

3.1. Energetics of the Fullerenes. Let us first consider the larger fullerenes Au_{50} and Au_{72}. The lowest energy hollow form of Au_{50} has D_{6d} symmetry,[5] while Au_{72} has chiral I symmetry.[6] For comparison, we optimized space-filling isomers, using the structures proposed by Doye and Wales[31] as starting points. Table 1 shows the relative energies between the hollow and compact forms of Au_{50} and Au_{72}. When a functional of sufficient quality is employed, both Au_{50} and Au_{72} are seen to clearly favor compact structures, and neither of these larger fullerenes are expected to be stable in free form.

Indirectly, Table 1 corroborates the stabilizing effect of spherical aromaticity; the hollow ions are even more unstable, with the exception of Au_{72}^-. By altering the valence electron count, the $2(N + 1)^2$ rule is no longer fulfilled and the stabilization borne of aromaticity weakened. Here, we note the connection to the nodeless spherical jellium model, recently reviewed by Häkkinen.[32] In the spherical jellium model, a concept common within the physics community,[33−36] compact metal clusters with valence electron counts equal to specific "magic numbers", corresponding to shell closings, exhibit enhanced stability, not unlike rare gas atoms.[3,37] By excluding shells with radial nodes, which cannot be accommodated by a hollow cluster, the resulting "magic" valence electron numbers are identical to those of the $2(N + 1)^2$ rule for spherical aromaticity; both are based on the same underlying principles, even if aromaticity is not traditionally associated with the delocalized electrons of jellium. Thus, altering the valence electron count is naturally unfavorable within both models.

Next, we turn to Au_{32}. So far, the neutral form of the fullerene has stood the test of time, and no lower energy isomers have been predicted. Jalbout et al.[38] have reported the most stable competing isomer to date. They also suggested that this isomer, here denoted "J10", was the most stable form for the cation and anion. Table 2 shows the energy difference between the fullerene and "J10", computed at TPSS level. Spin−orbit (SO) corrections and relative zero-point vibrational energies (ZPE) are accounted for.

At zero Kelvin, the hollow form of the anion lies significantly higher in energy compared to the compact isomer, while the highly symmetric neutral (I_h) and cationic (T_h) fullerenes are stable. Entropy will, however, collapse the cages at higher temperature.[9] The computed cross-over temperature to lumpiness, that is, the point where the free energy ΔG becomes lower for the space-filling isomer, is 285 K for the cation and 299 K for neutral Au_{32}. These temperatures should be considered as rough guidelines, due to their sensitivity toward the approximations involved.

Contrary to suggestions in the literature,[39] spin−orbit corrections are seen to have a significant effect on the relative energies. For neutral Au_{32}, SO favors the compact form. The same observation was made for smaller Au anions[11] and attributed to the SO splitting of orbitals that would enhance the Au−Au interaction. This would favor compact structures with more bonding neighbors. Both ions seem to contradict this observation, however, with SO favoring the fullerenic form. Perhaps the picture of enhanced bonding due to orbital splitting is too simplistic. Another explanation is also possible. As shown below, the aromaticity of especially the ions is quite sensitive to relativistic effects. It is therefore plausible that the SO interaction enhances the aromaticity of the ions (or rather, in the case of the anion, dampens the degree of antiaromaticity), with a concomitant increase in stability.

A brief discussion on the performance of other common functionals oft used in the study of gold clusters is in place, to underline the importance of employing good functionals even for qualitative energy differences. As a representative example, the stability of anionic Au_{32}^- in its fullerenic vs "J10" compact form was calculated with the widely popular PBE and Becke-Perdew (BP86)[40,41] functionals, using the def2-QZVPP basis set. The overstabilization of the hollow form is substantial. The electronic energy differences (without SO) in favor of the fullerene are 94 and 139 kJ/mol at PBE and BP86 levels, respectively, in severe contradiction with experiment.[9] We note that the use of too small a basis set, which strongly favors compact isomers,[11] can in fortuitous circumstances partly cancel the serious short-comings of a specific functional. The PBE functional modified for solids and surfaces (PBEsol)[27] and even the local spin density approximation (LSDA)[42] fare much better. LSDA, well-known to overestimate Au−Au interactions and bonding in general, favors the compact anion by 42 kJ/mol. PBEsol, shown to be accurate for smaller gold anions,[11] predicts the fullerenic forms to be slightly more stable than TPSS; compact Au_{32}^- is favored by only 6 kJ/mol at the PBEsol level.

3.2. Spherical Aromaticity and Magnetic Shielding. So far in the discussion, the evidence for spherical aromaticity has been circumstantial, based on the relatively high stability of the neutral forms compared to the ions of the fullerenes. The magnetic shieldings at the cage centers provide an estimate of the degree of spherical aromaticity. This nucleus-independent chemical shift (NICS) test,[20] although not a quantitative measure of aromaticity,[43] does correlate well with the aromatic degree and the strength of the sphere currents in, for example, carbon fullerenes,[44] as the reference point is located sufficiently far from any atom. In general, the magnetic shielding inside a spherical cage is constant and depends on the current strengths and radius of the system.[45] Table 3 shows the NICS values for various clusters. To assess the role of relativity, NICS values were also calculated for Ag_{32}, as well as using a nonrelativistic approach.

Neutral Au_{32} is highly aromatic, with a NICS value of −81 ppm. Removal of an electron decreases the aromaticity significantly; the NICS of the cation is halved. For the anion the

Golden Fullerene Stability

J. Phys. Chem. C, Vol. 112, No. 49, 2008 **19313**

TABLE 3: NICS Values (in ppm) at the Cage Centers of the Hollow Structures[a]

	Au_{32}	Au_{32}^+	Au_{32}^-	Ag_{32}	Au_{50}	Au_{72}
symmetry	I_h	T_h	C_{2h}	I_h	D_{6d}	I
SR	−81	−42	+199	−83	−89[b]	−111[b]
NR	−86	−19		−88	−82	

[a] Both scalar relativistic (SR) and non-relativistic (NR) values are reported. Computed at PBE level, with the Stuttgart 1990 pseudopotential and the corresponding valence basis set,[17] except where noted. [b] From ref 6; BP86 level.

change is even more pronounced: The cluster turns highly antiaromatic. The NICS values correlate well with cluster stability; the less aromatic, the less stable. Put in another way, neutral Au_{32} has an anomalously high ionization potential and low electron affinity. As a side note, this high dependence of the structure on charge state was recently observed also for boron clusters, where reducing neutral B_{20} destroys the highly symmetric double ring structure.[46] One can also see the large effect of relativity on the shielding at the centers. For the neutral, the relativistic effects are small (or canceling); also the hypothetical Ag_{32} fullerene shields its center equally efficiently. For the ions, the situation is quite different. In a nonrelativistic world, the cation would be much less aromatic still, while the anion would turn highly aromatic.

As noted by Karttunen et al.,[6] aromaticity increases with the size of the cage. For the larger fullerenes Au_{50} and Au_{72}, the stabilizing effect, although stronger than for Au_{32}, is however not enough to overcome the increasingly unfavorable lack of bonding neighbors compared to compact forms. Thus, Au_{32} is most likely the largest single-wall golden fullerene that could be synthesized in free form. The existence of larger, multiwall hollow structures as originally proposed[1] is not ruled out.

3.3. Doping the Fullerene. From an application point-of-view, the ability to strongly alter the structure of the fullerene by injection (or removal) of electrons is interesting. The relatively low thermal stability of the cages could perhaps also be exploited. These properties pose a challenge for experimental detection of fullerenic Au_{32}, however. A way of detecting the hollow neutral form would be via the large chemical shift of, say, an endohedrally enclosed rare gas atom, or, as recently shown,[47] by vibrational spectroscopy. In any case, for mass separation of the clusters via mass spectroscopy, a net charge is required, at least initially. As the temperatures of the cluster sources can be high, inflating an initially compact isomer to the lower energy cage form after cooling is expected to have a high kinetic barrier, as several Au−Au bonds would have to be broken in the process. In an attempt to overcome these complications, we propose an alternative approach: Doping Au_{32} with an ion.

So as not to collapse the hollow structure, the ion should interfere as little as possible with the stability of the cluster. As some charge flow will occur between the ion and the gold cage, a cation is expected to be a better choice than an anion. Due to their low ionization energies, alkali metals should be especially suitable. We have chosen sodium as the example cation, inspired by the recent experimental preparation of bimetallic Au−Na clusters.[48] Naturally, other ions would also be possible.

The stability of $[Au_{32}Na]^+$ was investigated as follows. To the fullerene, a sodium cation was inserted both endohedrally and exohedrally, after which the geometry was optimized. To compare with a compact form, we added Na^+ to the "J10" structure.[38] Several different positions were tested. With a well relaxed compact form as a starting point, this provides a
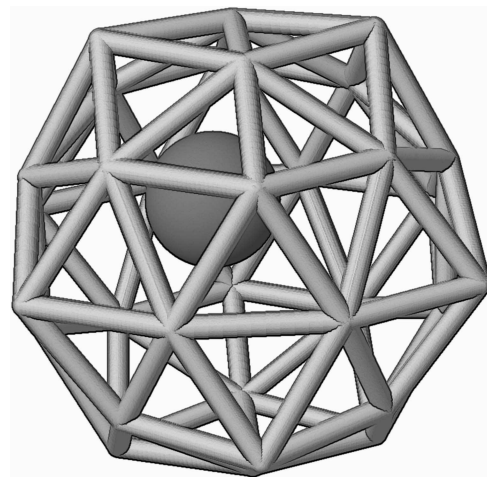
Figure 1. Structure of endohedral $[Na@Au_{32}]^+$.

TABLE 4: Relative Energies (in kJ/mol) of $[Au_{32}Na]^{+a}$

	$[Na@Au_{32}]^+$	$[Na@Au_{32}]^+$	$[Na⊕Au_{32}]^+$	$[Na⊕J10]^+$
symmetry	C_s	I_h	C_s	C_1
SR	0	+10.01	+46.92	+46.56
SO	0	−1.02	+2.09	−10.83
ZPE	0	−1.00	+0.86	−1.46
total	0	+8.0	+49.9	+34.3
ν_1	13	$i74$	33	22
Na−Au	321	391	297	309
gap	1.56	1.47	1.40	0.36
NICS	−81		−80	
δ_{Na}	35	45	−82	−63

[a] Values for endohedrally doped fullerene ($[Na@Au_{32}]^+$; C_s, off-center site; I_h, at center), exohedrally doped fullerene ($[Na⊕Au_{32}]^+$), and a compact isomer ($[Na⊕J10]^+$). The lowest vibrational frequencies (ν_1, in cm^{-1}), shortest Na−Au bond lengths (Na−Au, in pm), the HOMO−LUMO gaps (gap, in eV), NICS values (in ppm), and Na shielding constants relative to Na^+ (δ_{Na}, in ppm) are also shown.

reasonable estimate of stability, although we emphasize that a comprehensive investigation of the conformation space was not performed; for a bimetallic cluster this would be extremely expensive. We find that for the compact "J10" derivative, sodium prefers to stay attached to the outside of the cluster. For the fullerene, the endohedral form (see Figure 1) is preferred over the exohedral. Table 4 shows the relative energies of these isomers.

The stability of the endohedral $[Na@Au_{32}]^+$ fullerene with respect to the compact form is at least as high as in the case of the pure gold clusters. The two lowest vibrational frequencies, both computed at 13 cm^{-1}, correspond to Na motion inside the cage, indicating that it is quite loosely bound. Moving the sodium to the midpoint of the cage only raises the energy by 8 kJ/mol, confirming the weak bonding, and relatively free endohedral mobility of sodium (preliminary studies indicate that the larger alkali metals actually form truly I_h symmetrical doped cages). Further, the gap between the highest occupied molecular orbital (HOMO) and the lowest unoccupied molecular orbital (LUMO) is almost identical to that of the 24-carat fullerene (1.58 eV at TPSS level). The shortest Au−Na bond length is 321 pm, appreciably longer than in the exohedral and compact isomers. Indeed, aromaticity is not destroyed as can be seen from the NICS value (calculated at the midpoint between Na and the far side of the cage). The shielding constants of sodium in the Au_{32} cage are larger than for the free Na^+ ion (623 ppm)
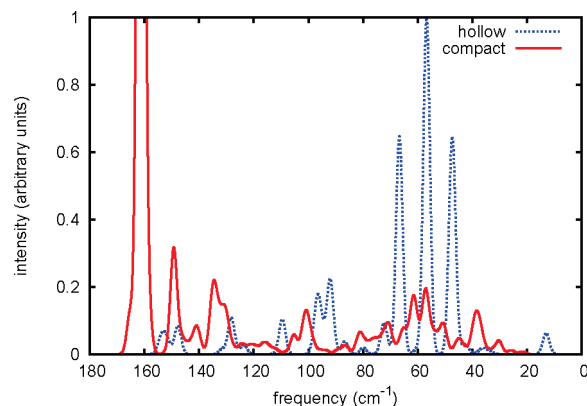
Figure 2. Simulated vibrational spectra of the hollow $[Na@Au_{32}]^+$ (dotted blue line) and compact $[Na{\oplus}J10]^+$ (full red line) isomers. For the compact isomer the most intense transition at $161\ cm^{-1}$ goes outside the picture, peaking at a value of 4.

and very similar for the two sites, indicating a smooth shielding hypersurface for Na within this miniature magnetic Faraday cage.[1] The increase of σ by 35 or 45 ppm as compared to free Na^+ corresponds to roughly one-half of the NICS of the empty cage. In contrast, the exohedral Na^+ behaves in the expected way: intermolecular interactions break the spherical symmetry of the ion and cause the onset of the negative, paramagnetic shielding term. The concomitant decrease of $\sigma(Na)$ takes place both for the open and compact Au_{32} structures.

Another very attractive property of the doped fullerene is its significantly enhanced thermal stability. The cross-over to the compact isomer is computed to take place at temperatures well over 5000 K. The bimetallic cluster is thus a promising candidate for synthesis. The increased stability also bodes well for functionalization of the fullerene via other types of endohedral doping. Further, measurable physical properties are expected to be very different for the hollow form, so its identification should be straightforward. This is exemplified by the sodium magnetic shielding and the vibrational frequencies, where the intense peaks are located at opposite sides of the spectrum for the hollow and compact forms, see Figure 2. It can be noted that although strictly only C_s symmetric, cage-like $[Na@Au_{32}]^+$ still exhibits a very clean spectrum; several of the peaks are grouped very close to each other, in contrast to the much more spread out spectrum of the truly low-symmetric compact form.

4. Conclusions

We have reinvestigated the stability of the spherically aromatic golden fullerenes, using reliable relativistic quantum chemical methods. We showed that only cationic and neutral Au_{32} are stable compared to alternative structures, providing a clear focus for synthesis. Although the stronger aromaticity of the larger fullerenes implies a stronger stabilizing effect, it cannot overcome the disadvantage of increasingly fewer average number of bonding partners. The loss of spherical aromaticity destabilizes the ions, especially the anion, in agreement with experiment.[9] We have proposed a stable doped form, $[Na@Au_{32}]^+$, as a promising candidate for experimental confirmation of the hollow structure.

References and Notes

(1) Johansson, M. P.; Sundholm, D.; Vaara, J. Au_{32}: A 24-Carat Golden Fullerene. *Angew. Chem., Int. Ed.* **2004**, *43*, 2678–2681.

(2) Gu, X.; Ji, M.; Wei, S. H.; Gong, X. G. Au_N clusters ($N = $ 32,33,34,35): Cagelike structures of pure metal atoms. *Phys. Rev. B* **2004**, *70*, 205401.

(3) Hirsch, A.; Chen, Z.; Jiao, H. Spherical Aromaticity in I_h Symmetrical Fullerenes: The $2(N+1)^2$ Rule. *Angew. Chem., Int. Ed.* **2000**, *39*, 3915–3917.

(4) Wang, J.; Jellinek, J.; Zhao, J.; Chen, Z.; King, R. B.; von Ragué Schleyer, P. Hollow Cages versus Space-Filling Structures for Medium-Sized Gold Clusters: The Spherical Aromaticity of the Au_{50} Cage. *J. Phys. Chem. A* **2005**, *109*, 9265–9269.

(5) Tian, D.; Zhao, J.; Wang, B.; King, R. B. Dual Relationship between Large Gold Clusters (Antifullerenes) and Carbon Fullerenes: A New Lowest-Energy Cage Structure for Au_{50}. *J. Phys. Chem. A* **2007**, *111*, 411–414.

(6) Karttunen, A. J.; Linnolahti, M.; Pakkanen, T. A.; Pyykkö, P. Icosahedral Au_{72}: a predicted chiral and spherically aromatic golden fullerene. *Chem. Commun.* **2008**, 465–467.

(7) Walter, M.; Häkkinen, H. A hollow tetrahedral cage of hexadecagold dianion provides a robust backbone for a tuneable sub-nanometer oxidation and reduction agent *via* endohedral doping. *Phys. Chem. Chem. Phys.* **2006**, *8*, 5407–5411.

(8) Bulusu, S.; Li, X.; Wang, L.-S.; Zeng, X. C. Evidence of hollow golden cages. *Proc. Natl. Acad. Sci. U.S.A.* **2006**, *103*, 8326–8330.

(9) Ji, M.; Gu, X.; Li, X.; Gong, X.; Li, J.; Wang, L.-S. Experimental and Theoretical Investigation of the Electronic and Geometrical Structures of the Au_{32} Cluster. *Angew. Chem., Int. Ed.* **2005**, *44*, 7119–7123.

(10) Oila, M. J.; Koskinen, A. M. P. Chirally modified gold nanoparticles: nanostructured chiral ligands for catalysis. *ARKIVOC* **2006**, *15*, 76–83.

(11) Johansson, M. P.; Lechtken, A.; Schooss, D.; Kappes, M. M.; Furche, F. The 2D-3D transition of gold cluster anions resolved. *Phys. Rev. A* **2008**, *77*, 053202.

(12) Scherbaum, F.; Grohmann, A.; Huber, B.; Krüger, C.; Schmidbaur, H. "Aurophilicity" as a Consequence of Relativistic Effects: The Hexakis(triphenylphosphaneaurio)methane Dication $[(Ph_3PAu)_6C]^{2+}$. *Angew. Chem., Int. Ed. Engl.* **1988**, *27*, 1544–1546.

(13) Tao, J.; Perdew, J. P.; Staroverov, V. N.; Scuseria, G. E. Climbing the Density Functional Ladder: Nonempirical Meta-Generalized Gradient Approximation Designed for Molecules and Solids. *Phys. Rev. Lett.* **2003**, *91*, 146401.

(14) Grimme, S. Semiempirical GGA-Type Density Functional Constructed with a Long-Range Dispersion Correction. *J. Comput. Chem.* **2006**, *27*, 1787–1799.

(15) Furche, F.; Perdew, J. P. The performance of semilocal and hybrid density functionals in 3 *d* transition-metal chemistry. *J. Chem. Phys.* **2006**, *124*, 044103.

(16) Weigend, F.; Ahlrichs, R. Balanced basis sets of split valence, triple-zeta valence and quadruple-ζ valence quality for H to Rn: Design and assessment of accuracy. *Phys. Chem. Chem. Phys.* **2005**, *7*, 3297–3305.

(17) Andrae, D.; Häußerman, U.; Dolg, M.; Stoll, H.; Preuß, H. Energy-adjusted *ab initio* pseudopotentials for the second and third row transition elements. *Theor. Chim. Acta* **1990**, *77*, 123–141.

(18) Perdew, J. P.; Burke, K.; Ernzerhof, M. Generalized Gradient Approximation Made Simple. *Phys. Rev. Lett.* **1996**, *77*, 3865–3868.

(19) Figgen, D.; Rauhut, G.; Dolg, M.; Stoll, H. Energy-consistent pseudopotentials for group 11 and 12 atoms: adjustment to multi-configuration Dirac-Hartree-Fock data. *Chem. Phys.* **2005**, *311*, 227–244.

(20) von Ragué Schleyer, P.; Maerker, C.; Dransfeld, A.; Jiao, H.; van Eikema Hommes, N. J. R. Nucleus-Independent Chemical Shifts: A Simple and Efficient Aromaticity Probe. *J. Am. Chem. Soc.* **1996**, *118*, 6317–6318.

(21) Schäfer, A.; Huber, C.; Ahlrichs, R. Fully optimized contracted Gaussian basis sets of triple-zeta valence quality for atoms Li to Kr. *J. Chem. Phys.* **1994**, *100*, 5829–5835.

(22) Ahlrichs, R.; Bär, M.; Häser, M.; Horn, H.; Kölmel, C. Electronic structure calculations on workstation computers: The program system Turbomole. *Chem. Phys. Lett.* **1989**, *162*, 165–169.

Golden Fullerene Stability

J. Phys. Chem. C, Vol. 112, No. 49, 2008 **19315**

(23) Treutler, O.; Ahlrichs, R. Efficient molecular numerical integration schemes. *J. Chem. Phys.* **1995**, *102*, 346–354.

(24) Eichkorn, K.; Treutler, O.; Öhm, H.; Häser, M.; Ahlrichs, R. Auxiliary basis sets to approximate Coulomb potentials. *Chem. Phys. Lett.* **1995**, *240*, 283–290.

(25) von Arnim, M.; Ahlrichs, R. Geometry optimization in generalized natural internal coordinates. *J. Chem. Phys.* **1999**, *111*, 9183–9190.

(26) Sierka, M.; Hogekamp, A.; Ahlrichs, R. Fast evaluation of the Coulomb potential for electron densities using multipole accelerated resolution of identity approximation. *J. Chem. Phys.* **2003**, *118*, 9136–9148.

(27) Perdew, J. P.; Ruzsinszky, A.; Csonka, G. I.; Vydrov, O. A.; Scuseria, G. E.; Constantin, L. A.; Zhou, X.; Burke, K. Restoring the Density-Gradient Expansion for Exchange in Solids and Surfaces. *Phys. Rev. Lett.* **2008**, *100*, 136406.

(28) Kendall, R. A.; Aprà, E.; Bernholdt, D. E.; Bylaska, E. J.; Dupuis, M.; Fann, G. I.; Harrison, R. J.; Ju, J.; Nichols, J. A.; Nieplocha, J.; Straatsma, T. P.; Windus, T. L.; Wong, A. T. High performance computational chemistry: An overview of NWChem a distributed parallel application. *Comput. Phys. Commun.* **2000**, *128*, 260–283.

(29) Frisch, M. J.; et al. *Gaussian 03*, revision C.02; Gaussian, Inc.: Wallingford, CT, 2004.

(30) Eichkorn, K.; Weigend, F.; Treutler, O.; Ahlrichs, R. Auxiliary basis sets for main row atoms and transition metals and their use to approximate Coulomb potentials. *Theor. Chem. Acc.* **1997**, *97*, 119–124.

(31) Doye, J. P. K.; Wales, D. J. Global minima for transition metal clusters described by Sutton-Chen potentials. *New J. Chem.* **1998**, *22*, 733–744.

(32) Häkkinen, H. Atomic and electronic structure of gold clusters: understanding flakes, cages and superatoms from simple concepts. *Chem. Soc. Rev.* **2008**, *37*, 1847–1859.

(33) Knight, W. D.; Clemenger, K.; de Heer, W. A.; Saunders, W. A.; Chou, M. Y.; Cohen, M. L. Electronic Shell Structure and Abundances of Sodium Clusters. *Phys. Rev. Lett.* **1984**, *52*, 2141–2143.

(34) Khanna, S. N.; Jena, P. Assembling Crystals from Clusters. *Phys. Rev. Lett.* **1992**, *69*, 1664–1667.

(35) de Heer, W. A. The physics of simple metal clusters: experimental aspects and simple models. *Rev. Mod. Phys.* **1993**, *65*, 611–676.

(36) Brack, M. The physics of simple metal clusters: self-consistent jellium model and semiclassical approaches. *Rev. Mod. Phys.* **1993**, *65*, 677–732.

(37) Reiher, M.; Hirsch, A. From Rare Gas Atoms to Fullerenes: Spherical Aromaticity Studied From the Point of View of Atomic Structure Theory. *Chem. Eur. J.* **2003**, *9*, 5442–5452.

(38) Jalbout, A. F.; Contreras-Torres, F. F.; Pérez, L. A.; Garzón, I. L. Low-Symmetry Structures of Au_{32}^Z ($Z = +1,0,-1$) Clusters. *J. Phys. Chem. A* **2008**, *112*, 353–357.

(39) Xiao, L.; Wang, L. From planar to three-dimensional structural transition in gold clusters and the spin-orbit coupling effect. *Chem. Phys. Lett.* **2004**, *392*, 452–455.

(40) Becke, A. D. Density-functional exchange-energy approximation with correct asymptotic behavior. *Phys. Rev. A* **1988**, *38*, 3098–3100.

(41) Perdew, J. P. Density-functional approximation for the correlation energy of the inhomogeneous electron gas. *Phys. Rev. B* **1986**, *33*, 8822–8824.

(42) Perdew, J. P.; Wang, Y. Accurate and simple analytic representation of the electron-gas correlation energy. *Phys. Rev. B* **1992**, *45*, 13244–13249.

(43) Lazzeretti, P. Assessment of aromaticity *via* molecular response properties. *Phys. Chem. Chem. Phys.* **2004**, *6*, 217–223.

(44) Johansson, M. P.; Jusélius, J.; Sundholm, D. Sphere Currents of Buckminsterfullerene. *Angew. Chem., Int. Ed.* **2005**, *44*, 1843–1846.

(45) Lounila, J.; Ala-Korpela, M.; Jokisaari, J.; Savolainen, M. J.; Kesäniemi, Y. A. Effects of orientational order and particle size on the NMR line positions of lipoproteins. *Phys. Rev. Lett.* **1994**, *72*, 4049–4052.

(46) Kiran, B.; Bulusu, S.; Zhai, H.-J.; Yoo, S.; Zeng, X. C.; Wang, L.-S. Planar-to-tubular structural transition in boron clusters: B_{20} as the embryo of single-walled boron nanotubes. *Proc. Natl. Acad. Sci. U.S.A.* **2005**, *102*, 961–964.

(47) Gruene, P.; Rayner, D. M.; Redlich, B.; van der Meer, A. F. G.; Lyon, J. T.; Meijer, G.; Fielicke, A. Structures of Neutral Au_7, Au_{19}, and Au_{20} Clusters in the Gas Phase. *Science* **2008**, *321*, 674–676.

(48) Cui, L.-F.; Lin, Y.-C.; Sundholm, D.; Wang, L.-S. A Photoelectron Spectroscopic and Computational Study of Sodium Auride Clusters, $Na_nAu_n^-$ ($n = 1-3$). *J. Phys. Chem. A* **2007**, *111*, 7555–7561.